On the variational computation of a large number of vibrational energy levels and wave functions for medium-sized molecules

Edit Mátyus,[1] Ján Šimunek,[1,2] and Attila G. Császár[1,a)]
[1]*Laboratory of Molecular Spectroscopy, Institute of Chemistry, Eötvös University, P.O. Box 32, H-1518 Budapest 112, Hungary*
[2]*Department of Inorganic Chemistry, Faculty of Natural Sciences, Comenius University, Mlynská dolina CH2, SK-84215 Bratislava, Slovakia*

(Received 20 March 2009; accepted 7 July 2009; published online 18 August 2009)

In a recent publication [J. Chem. Phys. **127**, 084102 (2007)], the nearly variational DEWE approach (DEWE denotes Discrete variable representation of the Watson Hamiltonian using the Eckart frame and an Exact inclusion of a potential energy surface expressed in arbitrarily chosen coordinates) was developed to compute a large number of (ro)vibrational eigenpairs for medium-sized semirigid molecules having a single well-defined minimum. In this publication, memory, CPU, and hard disk usage requirements of DEWE, and thus of any DEWE-type approach, are carefully considered, analyzed, and optimized. Particular attention is paid to the sparse matrix-vector multiplication, the most expensive part of the computation, and to rate-determining steps in the iterative Lanczos eigensolver, including spectral transformation, reorthogonalization, and restart of the iteration. Algorithmic improvements are discussed in considerable detail. Numerical results are presented for the vibrational band origins of the $^{12}CH_4$ and $^{12}CH_2D_2$ isotopologues of the methane molecule. The largest matrix handled on a personal computer during these computations is of the size of $(4\cdot10^8)\times(4\cdot10^8)$. The best strategy for determining vibrational eigenpairs depends largely on the actual details of the required computation. Nevertheless, for a usual scenario requiring a large number of the lowest eigenpairs of the Hamiltonian matrix the combination of the thick-restart Lanczos method, shift-fold filtering, and periodic reorthogonalization appears to result in the computationally most feasible approach. © *2009 American Institute of Physics*.
[DOI: 10.1063/1.3187528]

I. INTRODUCTION

The detailed line-by-line information provided by high-resolution rovibrational spectroscopic experiments for small- to medium-sized molecules, such as water, carbon dioxide, ozone, and methane is a requisite for several scientific and engineering applications and thus has been included in information systems.[1] The information in these databases has been used in the modeling of planetary atmospheres (including that of Earth) and in combustion research. Experimental and empirical approaches yield accurate but extremely incomplete spectroscopic information.[2] On the other hand, state-of-the-art (nearly) variational quantum chemical approaches can result in the complete spectral information, but the accuracy lacks significantly behind that of experiments. Therefore, the experimental and computational approaches are complementary to a large extent and must live together for the foreseeable future, and further development of accurate computational quantum chemical techniques is not only desirable but also highly useful.

Due to recent developments in electronic structure techniques and fitting algorithms, precise representations of the potential energy surface (PES)[3,4] and the electric dipole moment surface (DMS)[5] can be constructed for small- to medium-sized molecules. Upon the numerically exact solution of the nuclear motion problem using such accurate (semi)global PESs, rovibrational energy levels are computed, which may approach spectroscopic accuracy. Using the corresponding wave functions and the DMS, transition intensities and thus, in principle, a complete rovibrational spectrum can be generated. In the majority of cases, the accuracy of variationally computed energy levels does not exceed that of experiments.[2] On the other hand, the accuracy of theoretical transition intensities can often compete with that of the experimental data. Shortly, the most important applications of variational nuclear motion methods in spectroscopy involve the computation of many (hundreds and thousands of) energy levels, wave functions, and transition intensities.

The precise computation of (nearly) complete rovibrational spectra (positions and intensities) of medium-sized molecules is still an extremely challenging task requiring sophisticated algorithms and their efficient implementation. The viable protocols can be classified as belonging to at least three classes. The first class of feasible variational (ro)vibrational approaches involves tailor-made Hamiltonians and computer programs. These programs are suitable for a given number of nuclei and bonding arrangement and use an analytic kinetic energy operator.[6–14] Obviously, there have been attempts to use universally defined sets of coordinates and explicit kinetic energy operators based on them. This second class of methods involves spherical polar coordinates[15] or Watson's rectilinear internal coordinates[16] and the Eckart

a)Electronic mail: csaszar@chem.elte.hu.

frame.[17] The Watson Hamiltonian,[16] as it is usually called,[18–20] corresponds to the latter choice and has numerous implementations,[21–29] though seemingly only one of them[29] has, at present, the capability to perform a numerically exact computation of (ro)vibrational eigenpairs corresponding to a given PES for molecules with more than four nuclei. There have also been initiatives toward developing universal (ro)vibrational codes that are applicable to species with an arbitrary number of nuclei with user-defined body-fixed frames and internal coordinates.[30–33] This third class is based on a completely numerical approach for computing the Hamiltonian matrix and thus does not require the knowledge of the explicit form of the kinetic energy operator for different molecules and different frames and coordinates.

Each of the above approaches requires the diagonalization of (Hamiltonian) matrices in order to compute (ro)vibrational eigenvalues and eigenvectors. One strategy results in lower-dimensional but nonsparse and non-direct-product matrices. Other strategies, based on direct-product bases, produce often enormous dimensional but sparse matrices with a special structure. In order to compute the required many (thousands of) eigenvalues for medium-sized molecules, an iterative eigensolver (the usual choice is the Lanczos[34–36] technique) must be implemented, adapted specifically to the features and requirements of theoretical (ro)vibrational spectroscopy.

In a previous paper from two of the authors (Part I),[29] the representation of the vibrational part of the Watson Hamiltonian using the Eckart frame was discussed on a direct-product grid employing the discrete variable representation (DVR) and Hermite polynomials as a basis. Eigenvalues and eigenvectors were computed using a Lanczos eigensolver. The approach was called DEWE, standing for the Discrete variable representation of the Watson Hamiltonian using the Eckart frame and an Exact inclusion of a PES expressed in arbitrarily chosen coordinates. In this paper, we discuss considerable improvements in the eigenvalue and eigenvector determination with DEWE, which allows the computation of hundreds of eigenpairs of five-atomic molecules in a single run.

The structure of the manuscript is as follows. First, the known background theory of DEWE is summarized. Then, the most CPU-demanding part of the algorithm, the multiplication of the Hamiltonian matrix with a vector, is presented, which was not detailed in Part I. Computational requirements and scaling properties are also reviewed. Second, the possible spectral transformation techniques are discussed. This is important as the original Hamiltonian matrix is often transformed in order to map the required range of its spectrum to the largest eigenvalues of another matrix and/or to produce a matrix with specific spectral properties, which are expected to be more favorable for an iterative eigensolver. In the presented applications the lowest eigenvalues and corresponding eigenvectors are determined. The computation of interior eigenpairs are also considered, which could make the evaluation of thousands of eigenpairs a "trivially" parallel task. Third, the treatment of Lanczos vectors expanding the Krylov subspace is considered. Due to the finite precision arithmetic of the codes used for programming on digital computers, the orthogonality of the Lanczos vectors is maintained artificially. Sophisticated reorthogonalization techniques were adapted in order to minimize the CPU and most importantly the input/output (I/O) operations originating from the required reading and writing of the Lanczos vectors stored on the hard disk. In order to keep the storage requirements of the Lanczos vectors manageable, the iteration may be restarted periodically. The paper ends with applications of the DEWE code for the $^{12}CH_4$ and $^{12}CH_2D_2$ isotopologues of the five-atomic methane molecule.

II. BACKGROUND THEORY OF DEWE

In Part I, the DEWE approach was described in considerable detail. Nevertheless, it is necessary to recall the notation and certain features of the DEWE protocol in order to understand what follows in this article. In DEWE (a) the DVR of the Watson Hamiltonian, corresponding to Eckart's body-fixed frame[17] and Watson's rectilinear internal coordinates,[16] is employed using a direct-product Hermite-DVR grid and (b) vibrational energy levels and wave functions are obtained by computing the eigenpairs of the real symmetric Hamiltonian matrix by means of a Lanczos iterative eigensolver.

Watson's rectilinear internal coordinates are introduced as

$$Q_k = \sum_{i=1}^{N} \sum_{\alpha=x,y,z} \sqrt{m_i} l_{i\alpha k} (x_{i\alpha} - c_{i\alpha}), \quad k = 1, \ldots, 3N-6, \tag{1}$$

where m_i is the mass associated with the ith nuclei, $c_{i\alpha}$ are the reference coordinates, and $x_{i\alpha}$ are the instantaneous Cartesian coordinates in the Eckart frame. The usage of the Eckart frame and Watson's orthogonality requirement[16] imposes the following conditions on the elements $l_{i\alpha k}$ specifying the actual rectilinear internal coordinates:

$$\sum_{i=1}^{N} \mathbf{l}_{ik}^T \mathbf{l}_{il} = \delta_{kl}, \quad \sum_{i=1}^{N} \sqrt{m_i} \mathbf{l}_{ik} = \mathbf{0}, \quad \text{and} \quad \sum_{i=1}^{N} \sqrt{m_i} \mathbf{c}_i \times \mathbf{l}_{ik} = \mathbf{0}. \tag{2}$$

Upon any choice of $\mathbf{c}$ and $\mathbf{l}$ satisfying the requirements given in Eq. (2), the vibrational Hamiltonian can be written in the Watson form[16] as

$$\hat{H}^{\text{vib}} = \frac{1}{2} \sum_{\alpha\beta} \hat{\pi}_\alpha \mu_{\alpha\beta} \hat{\pi}_\beta + \frac{1}{2} \sum_{k=1}^{3N-6} \hat{P}_k^2 - \frac{\hbar^2}{8} \sum_{\alpha} \mu_{\alpha\alpha} + V, \tag{3}$$

where the quantities introduced have their usual meaning (see Part I).

Normalized Hermite polynomials, $H_j(q)$, are employed to construct a basis for the matrix representation of the Watson Hamiltonian. Instead of using spectral functions, the corresponding DVR functions are employed. Construction of the Hermite-DVR grid points and matrices of the derivative operators are discussed in detail in Part I.

Matrix representation of $\hat{H}^{\text{vib}}$ on a direct-product Hermite-DVR grid can be facilitated by introducing the truncated resolution of identity between $\hat{\pi}_\alpha$ and $\mu_{\alpha\beta}$ and between $\mu_{\alpha\beta}$ and $\hat{\pi}_\beta$,

$$\mathbf{H}^{\mathrm{vib}} = \frac{1}{2}\sum_{\alpha\beta} \boldsymbol{\pi}_\alpha \boldsymbol{\mu}_{\alpha\beta} \boldsymbol{\pi}_\beta + \frac{1}{2}\sum_{k=1}^{3N-6} \mathbf{P}_k^2 - \frac{\hbar^2}{8}\sum_{\alpha} \boldsymbol{\mu}_{\alpha\alpha} + \mathbf{V}, \quad (4)$$

where $\boldsymbol{\mu}_{\alpha\beta}(\alpha,\beta=x,y,z)$ and $\mathbf{V} \in \mathcal{R}^{\mathcal{N}\times\mathcal{N}}$ are diagonal matrices. $\mathcal{N}$ is the size of the direct-product grid, $\mathcal{N}=\Pi_{i=1}^{3N-6} N_i$, where N_i denotes the number of grid points corresponding to the ith vibrational degree of freedom. In order to compute eigenpairs of the symmetric Hamiltonian matrix given in Eq. (4) a Lanczos iterative eigensolver is employed in DEWE.

The Lanczos technique[34–36] is a widely used iterative method for the computation of a set of eigenvalues and eigenvectors of large (and often sparse), real symmetric matrices. Let us denote the matrix in question by $\mathbf{A} \in \mathrm{R}^{M\times M}$ and choose an initial vector $\mathbf{q}_1$ of norm unity. Set $\beta_0=0$, $\mathbf{q}_0=0$, and then the Lanczos iteration can be described as

Do $j=1,2,\ldots,m$
(a) $\mathbf{q}_{j+1}=\mathbf{A}\mathbf{q}_j$
(b) $\alpha_j=(\mathbf{q}_j,\mathbf{q}_{j+1})$
(c) $\mathbf{q}_{j+1}=\mathbf{q}_{j+1}-\alpha_j\mathbf{q}_j-\beta_{j-1}\mathbf{q}_{j-1}$
(d) $\beta_j=\|\mathbf{q}_{j+1}\|$ if $\beta_j=0$ then **Stop**
(e) $\mathbf{q}_{j+1}=\mathbf{q}_{j+1}/\beta_j$
End do

After step m the following recurrence is valid for the Lanczos vectors:

$$\mathbf{A}\mathbf{Q}_m = \mathbf{Q}_m\mathbf{T}_m + \beta_m\mathbf{q}_{m+1}\mathbf{e}_m^T, \quad (5)$$

where the columns of $\mathbf{Q}_m$ contain the first m Lanczos vectors, $\mathbf{e}_m$ is the last column of the identity matrix $\mathbf{I}_m$, and $\mathbf{T}_m=\mathbf{Q}_m^T\mathbf{A}\mathbf{Q}_m \in \mathcal{R}^{m\times m}$ is a symmetric tridiagonal matrix with the elements α_j $(j=1,\ldots,m)$ on the diagonal and β_j $(j=1,\ldots,m-1)$ below and above the diagonal. The eigenvalues of $\mathbf{T}_m$ are the Ritz values. If the eigenvectors of $\mathbf{T}_m$ are denoted by $\mathbf{y}_i$ $(i=1,2,\ldots,m)$, the vectors $\mathbf{v}_i=\mathbf{Q}_m\mathbf{y}_i$ are the Ritz vectors. The Ritz values and vectors are the Rayleigh–Ritz approximations to the eigenvalues and eigenvectors of $\mathbf{A}$ from the subspace spanned by the Lanczos vectors $\mathbf{Q}_m$ with typically $m \ll M$.

At this point, a couple of important properties of the Lanczos algorithm are worth emphasizing. First, the eigenvalues of $\mathbf{T}_m$ $(m=1,2,\ldots)$ converge to the largest eigenvalues of $\mathbf{A}$. Therefore, instead of introducing $\mathbf{H}^{\mathrm{vib}}$ directly in the Lanczos iteration, a spectral transformation is carried out using a filter function, $\mathbf{A}'=\mathcal{F}(\mathbf{A})$, so that the required eigenvalues of $\mathbf{A}$ are the largest eigenvalues of $\mathbf{A}'$. The required range is often the lowest end of the spectrum. Second, explicit knowledge of the matrix $\mathbf{A}$ is not required. Even if a spectral transformation step is introduced in the algorithm, only the multiplication of $\mathbf{A}$ with a vector is needed. Third, the Lanczos vectors remain orthogonal among each other only if exact arithmetics is used. Due to round-off errors, resulting from the use of finite arithmetics, the orthogonality is satisfied only at the beginning of the iteration. The loss of orthogonality results in copies of eigenvalues and spurious values in the computed spectrum. To avoid the computation of these annoying features, the orthogonality of Lanczos vectors must be artificially maintained.

III. MULTIPLICATION OF THE HAMILTONIAN MATRIX WITH A VECTOR

One of the prime features making iterative eigensolvers useful in the DEWE protocol is the fact that the Hamiltonian matrix of Eq. (4) does not need to be constructed explicitly; only its product with a vector is required. What makes DEWE applicable to larger computations is that the product of the Hamiltonian matrix, $\mathbf{H}^{\mathrm{vib}}$, with a vector, $\mathbf{x}$, is computed as

$$\mathbf{y} = \mathbf{H}^{\mathrm{vib}}\mathbf{x} = \frac{1}{2}\sum_{\alpha}\left(\boldsymbol{\pi}_\alpha\sum_{\beta}\boldsymbol{\mu}_{\alpha\beta}(\boldsymbol{\pi}_\beta\mathbf{x})\right) + \frac{1}{2}\sum_{k=1}^{3N-6}\mathbf{P}_k^2\mathbf{x} + \mathbf{V}'\mathbf{x}, \quad (6)$$

where the parentheses indicate the order of the operations, and

$$\mathbf{V}' = \mathbf{V} - \frac{\hbar^2}{8}\sum_{\alpha}\boldsymbol{\mu}_{\alpha\alpha}, \quad (7)$$

$$\mathbf{P}_k = -i\mathbf{I}_1\otimes\mathbf{I}_2\otimes\cdots\otimes\mathbf{I}_{k-1}\otimes\mathbf{D}_k^{[1]}\otimes\mathbf{I}_{k+1}\otimes\cdots\otimes\mathbf{I}_{3N-6} \in \mathcal{R}^{\mathcal{N}\times\mathcal{N}}, \quad (8)$$

$$\mathbf{P}_k^2 = \mathbf{I}_1\otimes\mathbf{I}_2\otimes\cdots\otimes\mathbf{I}_{k-1}\otimes\mathbf{D}_k^{[2]}\otimes\mathbf{I}_{k+1}\otimes\cdots\otimes\mathbf{I}_{3N-6} \in \mathcal{R}^{\mathcal{N}\times\mathcal{N}}, \quad (9)$$

and $k=1,2,\ldots,3N-6$. $\mathbf{I}_k \in \mathcal{R}^{N_k\times N_k}$ denotes a unit matrix; $\mathbf{D}_k^{[1]}$ and $\mathbf{D}_k^{[2]} \in \mathcal{R}^{N_k\times N_k}$ are the matrices of $\hbar\partial/\partial Q_k$ and $\hbar^2\partial^2/\partial Q_k^2$ in DVR. In Hermite-DVR $\mathbf{D}_k^{[1]}$ and $\mathbf{D}_k^{[2]}$ are antisymmetric and symmetric matrices, respectively. For convenience, let us introduce the notation $\mathfrak{N}_l=\Pi_{j=1}^{l-1}N_j$. It is also useful to introduce a composite index n that can be expressed as $n=1+\Sigma_{k=1}^{3N-6}(n_k-1)\mathfrak{N}_k$ using the subindices $(n_1,n_2,\ldots,n_{3N-6})$.

The matrix-vector multiplication algorithm is described on Scheme 1. This algorithm requires the storage of $10\mathcal{N}$ 64-bit real numbers. The multiplication with the matrices $\boldsymbol{\pi}_\alpha$ and $\mathbf{P}_k^2$ can be carried out only by using the ζ_{kl}^α elements, the quadrature points $\mathbf{q}$, and the $\mathbf{D}_l^{[1]}$ and $\mathbf{D}_k^{[2]}$ matrices, which have negligible storage requirements. The number of multiplicative operations is $(1+12D(D+1)+14DN')\mathcal{N}$, where $D=3N-6$, and N' is a representative number for the number of points along a vibrational degree of freedom $(N_1,N_2,\ldots,N_{3N-6}$ can have different values).

In the matrix-vector multiplication algorithm, the main loop is organized for the elements of the product vector, which is thus computed directly (not iteratively). This makes this algorithm straightforwardly parallelizable with OPENMP (Ref. 37) (as indicated on the sketch of the algorithm). The parallel speed-up on a SUPERMICRO server machine equipped with two quadcore Xeon processors is nearly ideal up to four cores. A graph showing the speed-up up to eight cores is presented in the supplementary material.[38]

Scheme 1

Initialization: Introduce $a \in \mathcal{R}$, $\mathbf{b} \in \mathcal{R}^{3\times 3}$, $\mathbf{c} \in \mathcal{R}^3$, $\mathbf{y}_\alpha \in \mathcal{R}^{\mathcal{N}}(\alpha = x,y,z)$, and set $a = 0$, $\mathbf{b} = \mathbf{0}$, $\mathbf{c} = \mathbf{0}$, $\mathbf{y}_\alpha = \mathbf{0}$ $(\alpha = x,y,z)$.

(a) Computation of the term $\left(\frac{1}{2}\sum_{k=1}^{3N-6} \mathbf{P}_k^2 + \mathbf{V}'\right)\mathbf{x}$

Do $n = 1,\ldots,\mathcal{N}$ ← OpenMP

$\mathbf{y}[n] = \mathbf{V}'[n]\ \mathbf{x}[n] + \sum_{k=1}^{3N-6}\sum_{j=1}^{N_k} \mathbf{D}_k^{[2]}[n_k,j]\ \mathbf{x}[n+(j-n_k)\mathfrak{N}_k)]$

End do

(b) Computation of the term $\frac{1}{2}\sum_{\alpha\beta} \boldsymbol{\pi}_\alpha \boldsymbol{\mu}_{\alpha\beta} \boldsymbol{\pi}_\beta \mathbf{x}$

Do $n = 1,\ldots,\mathcal{N}$ ← OpenMP

Do $l = 1,\ldots,3N-6$

$a = \sum_{j=1}^{N_l} \mathbf{D}_l^{[1]}[n_l,j]\ \mathbf{x}[n+(j-n_l)\mathfrak{N}_l]$

$\mathbf{y}_\alpha[n] = \mathbf{y}_\alpha[n] + \left(\sum_{k=1}^{3N-6} \zeta_{kl}^\alpha\ q[k,n_k]\right) a, \quad \alpha = x,y,z$

End do

End do

Do $n = 1,\ldots,\mathcal{N}$ ← OpenMP

$a = 0$

Do $l = 1,\ldots,3N-6$

$b_{\alpha\beta} = \sum_{j=1}^{N_l} \boldsymbol{\mu}_{\alpha\beta}[n+(j-n_l)\mathfrak{N}_l]\ \mathbf{y}_\beta[n+(j-n_l)\mathfrak{N}_l], \quad \alpha,\beta = x,y,z$

$c_\alpha = \sum_{j=1}^{N_l} \mathbf{D}_l^{[1]}[n_l,j]\ (b_{\alpha x} + b_{\alpha y} + b_{\alpha z}), \quad \alpha = x,y,z$

$a = a + \sum_\alpha \left(\sum_{k=1}^{3N-6} \zeta_{kl}^\alpha\ q[k,n_k]\right) c_\alpha$

End do

$\mathbf{y}[n] = \mathbf{y}[n] - a/2$

End do

IV. IMPROVEMENTS IN THE EIGENPAIR DETERMINATION

A. Spectral transformations

The conventional Lanczos algorithm converges to the largest eigenvalues of a matrix. The convergence rate of the Lanczos iteration is determined by the relative separation of the eigenvalues, $\eta_i = |E_{i+1} - E_i| / (E_{\max} - E_{\min})$.[39]

In order to compute the lowest or interior eigenvalues instead of the largest ones, the original matrix is transformed so that the required eigenvalues become the largest eigenvalues of the transformed matrix. There are several possibilities to set up such a spectral transformation.[40–42] The cost of the transformation and the spectral properties of the resultant matrix can be very different.

In the present work, polynomial, exponential, and shift-invert transformation techniques were studied. In Fig. 1 a pictorial overview is given about the different transformation techniques by visualizing the spectral properties of the transformed matrices with respect to the original spectrum. The relative separation η_i of the eigenvalues corresponding to the transformed matrices are given and discussed in detail in the supplementary material. In what follows the most important technical aspects are discussed separately for the different cases considered.

It is worth noting that the converged eigenvectors of the transformed and the original matrices are the same. If necessary, the eigenvalues of the original matrix E_i^0 can be recovered by computing the expectation value of the original matrix for the eigenvectors, e.g., $E_i^0 = \langle \mathbf{v}_i | \mathbf{H} | \mathbf{v}_i \rangle$.

1. Polynomial filtering

The family of polynomial spectral transformation techniques[43,44] can be written in general as

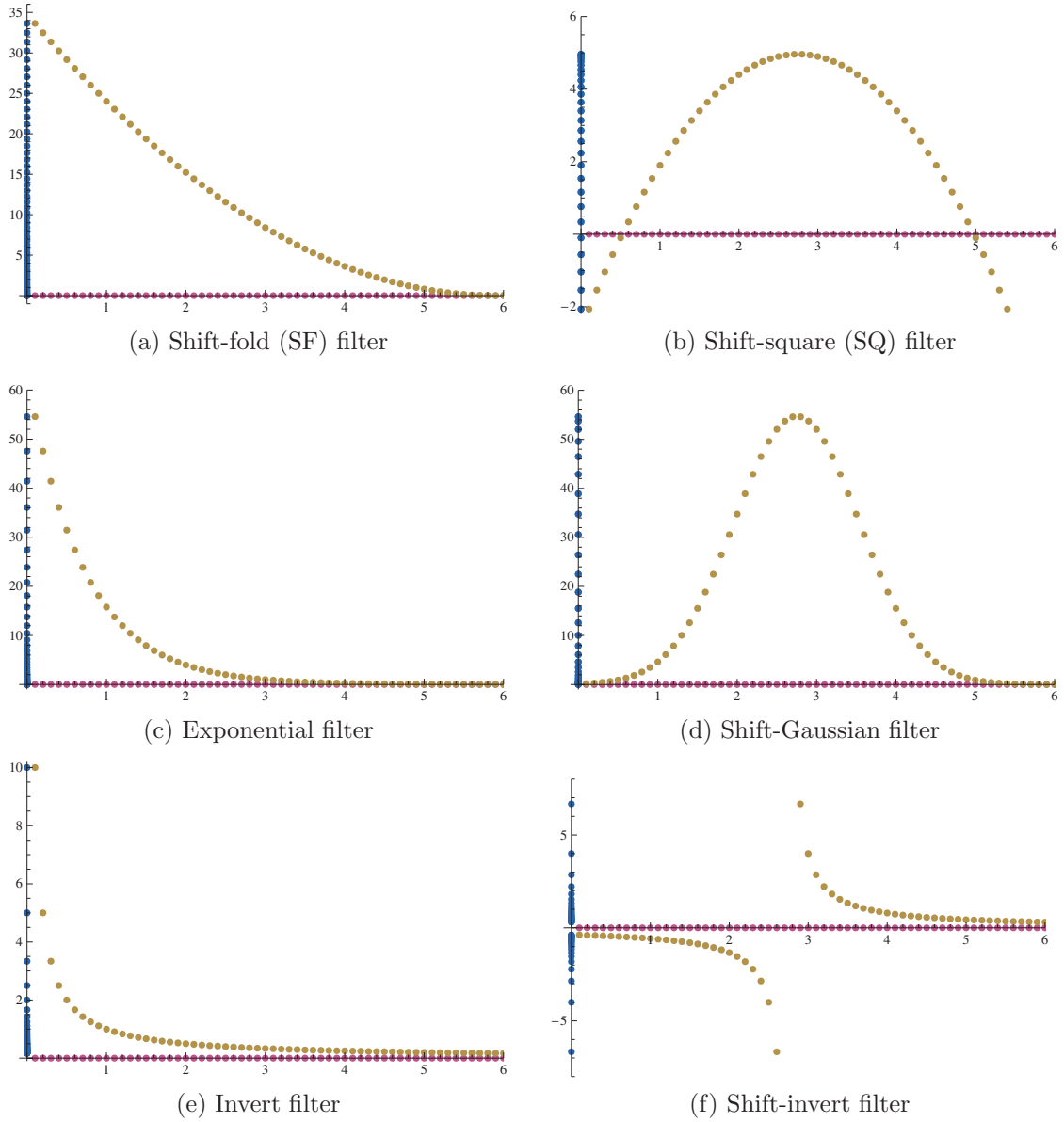

FIG. 1. Schematic representation of different spectral transformation techniques. Line positions of the original and transformed spectra are represented on the x- and y-axes (red and blue circles), respectively. The graphs of the transformation functions are also plotted at discrete points (brown circles) on the x-y plane. See the text for the mathematical definition of the filters presented on plots (a)–(f).

$$\mathcal{P}_n(\mathbf{H},\alpha,\kappa,\lambda) = [\lambda\mathbf{I} - \alpha(\mathbf{H}-\kappa\mathbf{I})^2]^{2n+1}, \quad n = 0,1,2,\ldots, \quad (10)$$

where the parameters α, κ, and λ can be tuned in order to map the required range of the original spectrum to the largest eigenvalues of $\mathcal{P}_n(\mathbf{H},\alpha,\kappa,\lambda)$. Two special cases of the family of polynomial filters given in Eq. (10) were used in the present work, a shift-fold (SF) and a shift-square (SQ) filtering. Polynomial filters can be easily implemented. The number of matrix-vector multiplications in a single spectral transformation step is $2(2n+1)$.

The largest eigenvalue of $\mathcal{P}_0(\mathbf{H},-1,E^0_{\max},0) = (\mathbf{H}-E^0_{\max}\mathbf{I})^2$ is the smallest eigenvalue of $\mathbf{H}$. Spectral properties of this SF transformation are visualized on Fig. 1(a). The relative separation of the eigenvalues corresponding to the transformed matrix (for details see the supplementary material) is increased by SF if $E^0_{\max} > 3E^0_{\min}$ and only the lowest eigenvalues of $\mathbf{H}$ are to be computed. Ideally, the relative separation of the eigenvalues of the SF-transformed matrix can be twice as large as that of the original one, i.e., $\eta_i^{\mathrm{SF}} \leq 2\eta_i^0$. Furthermore, the relative separation of the original spectrum η_i^0 can be increased by decreasing the largest eigenvalue of the original matrix, e.g., by means of an appropriate truncation of the direct-product grid. Upon the computation of the lowest levels, this further increases the relative separation of the eigenvalues of the transformed matrix as well, thus increasing the convergence rate of the Lanczos iteration. The largest eigenvalues of $\mathcal{P}_0(\mathbf{H},1,\kappa,\lambda) = \lambda\mathbf{I} - (\mathbf{H}-\kappa\mathbf{I})^2$ are the eigenvalues of $\mathbf{H}$ from the neighborhood of κ, where κ is a point from the required spectral range and $\lambda = \max[(\mathbf{H}-\kappa\mathbf{I})^2]/2$. Spectral properties of this transformation are visualized on Fig. 1(b). As apparent from Fig. 1(b), the high end of the transformed spectrum is very dense leading to slow convergence. One can demonstrate that the relative separation of the transformed eigenvalues is much smaller than that of the original ones for the interesting

spectral range. Furthermore, folding (squaring) the original spectrum around an interior point κ makes the transformed spectrum nearly doubly degenerate, which worsens the convergence of the Lanczos iteration.

2. Exponential filtering

Compared to the polynomial filters, the use of an exponential function can provide more advantageous spectral properties to the transformed matrix.[39,45,46] A family of exponential filters can be introduced as

$$\mathcal{T}_n(\mathbf{H},\alpha,\kappa) = e^{-\alpha[(\mathbf{H}-\kappa\mathbf{I})^n-\bar{\lambda}\mathbf{I}]/\Delta}, \quad n=1 \text{ or } 2, \tag{11}$$

where $\bar{\lambda}=(\lambda_{\max}+\lambda_{\min})/2$ and $\Delta=(\lambda_{\max}-\lambda_{\min})/2$, where the notations $\lambda_{\max}=\max[(\mathbf{H}-\kappa\mathbf{I})^n]$ and $\lambda_{\min}=\min[(\mathbf{H}-\kappa\mathbf{I})^n]$ were used.

Exponential functions of matrices can be dealt with efficiently by using a Chebyshev expansion, as suggested originally by Tal-Ezer and Kosloff[47] for the complex case and later adapted, for instance, by Yu and Nyman,[39,45,46] for real functions. Let us introduce the notation

$$f(\mathbf{H}) = \mathcal{T}_n(\mathbf{H},\alpha,\kappa); \tag{12}$$

then

$$f(\mathbf{H}) \approx \sum_{l=0}^{L} A_l T_l(\mathbf{H}'), \tag{13}$$

where $\mathbf{H}'=(\mathbf{H}-\bar{H})/\Delta H$, $\bar{H}=(E^0_{\max}+E^0_{\min})/2$, $\Delta H=(E^0_{\max}-E^0_{\min})/2$, $E^0_{\max}$ and $E^0_{\min}$ are the largest and smallest eigenvalues of $\mathbf{H}$, respectively, T_l is the lth Chebyshev polynomial of the first kind, and the expansion coefficients

$$A_l = \frac{2-\delta_{l0}}{\pi}\int_{-1}^{+1}\frac{f(E)T_l(E)}{\sqrt{1-E^2}}\mathrm{d}E \tag{14}$$

can be computed numerically by Gaussian quadrature. The accuracy of the expansion can be increased by including higher degree Chebyshev polynomials. In each transformation step, the number of multiplications of the original matrix with a vector is L, the largest degree of Chebyshev polynomials included in the expansion.

The largest eigenvalue of $\mathcal{T}_1(\mathbf{H},\alpha,0)=e^{-\alpha(\mathbf{H}-\bar{H}\mathbf{I})/\Delta}$ is the smallest eigenvalue of $\mathbf{H}$. As demonstrated on Fig. 1(c), the lowest end of the spectrum is mapped to the largest well-separated eigenvalues of the transformed spectrum. In principle, the relative separation of two close-lying levels can be increased to close to one (note that $0\leq\eta_i\leq 1$) by choosing an appropriately large α. In practice, however, the increasing number of terms in the expansion in Eq. (13) and the finite numerical representation can limit this possibility. Apart from the technical difficulties, the transformation $\mathcal{T}_1(\mathbf{H},\alpha,0)$, given in Eq. (11), allows to speed up the convergence of the Lanczos iteration by increasing α at the expense of an increase in the cost of the transformation. The larger α becomes, the higher the order of the terms to be kept in the Chebyshev expansion, resulting in more matrix-vector multiplications in a single transformation step.

The largest eigenvalues of $\mathcal{T}_2(\mathbf{H},\alpha,\kappa)=e^{-\alpha[(\mathbf{H}-\kappa\mathbf{I})^2-\bar{\lambda}\mathbf{I}]/\Delta}$ correspond to the eigenvalues closest to κ, an interior point in the original spectrum. The spectral properties of the transformed matrix are visualized on Fig. 1(d). Due to the exponential filter, the relative separation of close-lying eigenvalues could be increased to a value close to one by choosing a sufficiently large α. However, similar to the SQ case, due to the folding of the original spectrum, the transformed spectrum becomes nearly doubly degenerate, which worsens the convergence rate of the Lanczos iteration.

3. Shift-invert filtering

The required eigenvalues can be mapped into well-separated eigenvalues by shifting and inverting the original Hamiltonian matrix,[40]

$$\mathcal{I}_+(\mathbf{H},\kappa) = (\mathbf{H}-\kappa\mathbf{I})^{-1}, \tag{15}$$

$$\mathcal{I}_-(\mathbf{H},\kappa) = (\kappa\mathbf{I}-\mathbf{H})^{-1}. \tag{16}$$

The largest eigenvalues of $\mathcal{I}_+(\mathbf{H},\kappa)$ or $\mathcal{I}_-(\mathbf{H},\kappa)$ are the eigenvalues closest to κ but respectively larger or smaller than κ. The advantageous spectral properties of this filtering can be observed on Figs. 1(e) and 1(f).

In practice, $\mathcal{I}_+(\mathbf{H},\kappa)$ and $\mathcal{I}_-(\mathbf{H},\kappa)$ are introduced in the Lanczos iterations simply by means of matrix-vector multiplications, which can be computed by using iterative linear solvers, e.g., the conjugate gradient method (CGM), the generalized minimal residual method, or the quasi-minimum residual method.[36] In DEWE the CGM has been tested for the computation of the lowest end of the spectrum using a simple diagonal preconditioning.[48]

The cost of the transformation, which is determined by the number of multiplications done with the original matrix $\mathbf{H}$, strongly depends on the spectral properties of $\mathbf{H}$ and the spectral density of $\mathbf{H}$ around κ. Several applications and improvements in the transformation algorithm have been published;[49–52] however, construction of an efficient and in some sense black-box method, for instance, a method that is efficient for any spectral range of a rotation-vibration Hamiltonian matrix, still remains a challenging task. The spectral properties of the transformed matrix suggest that once such a shift-invert transformation is set up, the Lanczos iteration converges fast.

For the computation of the lowest eigenvalues, $\mathcal{I}_+(\mathbf{H},0)=(\mathbf{H})^{-1}$ can be used. The convergence rate can be improved if $\mathcal{I}_+(\mathbf{H},\kappa<E^0_{\min})=(\mathbf{H}-\kappa\mathbf{I})^{-1}$ is employed. For the computation of interior eigenvalues of $\mathbf{H}$, the $\mathcal{I}_+(\mathbf{H},\kappa)$ and $\mathcal{I}_-(\mathbf{H},\kappa)$ transformations can be used with $E^0_{\min}<\kappa<E^0_{\max}$. In contrast to the polynomial and exponential filters, here the original spectrum is not folded around the interior point κ; thus the inconvenient near double degeneracy is not introduced in the transformed spectrum.

This functional form was seemingly suggested for the computation of interior eigenvalues first in 1980.[40] Since then this filter has been recognized as the one that produces the most favorable spectral properties for the computation of a few eigenvalues. However, to carry out such a spectral transformation efficiently for any κ remains challenging.

To summarize this section, the choice of the spectral transformation is a rather delicate question, and the optimal choice seems to depend strongly on the application. By choosing an appropriate form of the spectral transformation, the required spectral range of the Hamiltonian matrix can be computed in the Lanczos iteration. In each Lanczos step the original matrix is transformed, which requires to carry out a certain number of multiplications of the Hamiltonian matrix with a vector. This matrix-vector multiplication is generally the most CPU-intensive part of the computation; thus, the number of matrix-vector multiplications required determines the "cost" of a specific spectral transformation. On the other hand, the spectral properties of matrices corresponding to different spectral transformation methods can be very different. The relative separation of eigenvalues of the matrix introduced in the Lanczos iteration strongly influences the convergence rate of the iteration.

To compute the few lowest or a few interior points of a spectrum, the most efficient spectral transformation technique seems to be the shift-invert filtering. Its cost, i.e., the number of matrix-vector multiplications, strongly depends on the spectral properties of the original matrix. This method becomes very expensive as the spectrum becomes dense in the required range.

Thus, a good strategy to compute several hundred eigenpairs is to settle for a less efficient but also less expensive spectral transformation method, such as the SF filter. The less efficient the spectral transformation method, the larger the iteration number of the Lanczos method and the larger the effort of the handling, i.e., storing and maintaining the orthogonality, of Lanczos vectors. Specific reorthogonalization and restarting methods, which have been found to perform the best in the computation of a large number of vibrational energy levels and wave functions, are discussed in the next section.

B. Building the Krylov subspace

In exact arithmetics Lanczos vectors are orthogonal by construction;[36,53] however, in the presence of round-off errors, this orthogonality is lost. Several approaches have been put forward to remedy this problem. The loss of orthogonality manifests itself in the appearance of spurious eigenvalues and copies of correct ones.

Cullum and Willoughby[35] suggested an algorithm that removed the extra and spurious eigenvalues *a posteriori* from the computed spectrum. This approach avoids the reorthogonalization of Lanczos vectors and thus their storage; however, the computation of spurious and extra levels wastes CPU time. Furthermore, if eigenvectors are also required, the storage of Lanczos vectors cannot be avoided. Wang and Carrington[54] used a method in which the orthogonality is not maintained among the Lanczos vectors and the technique suggested by Cullum and Willoughby was adapted for the computation of eigenvalues. If eigenvectors were also required, they were computed in a second run using Lanczos vectors.

In contrast to the approach used by Wang and Carrington, in DEWE we prefer to obtain eigenvalues and eigenvectors from a single calculation. To achieve this we store the Lanczos vectors, but in order to avoid redundant storage of information, (semi)orthogonality is maintained among the Lanczos vectors throughout the calculation. Lanczos vectors can be very large, and if many eigenpairs are required, a large number of such vectors must be stored (typically on the hard disk). Thus, efficient reorthogonalization algorithms and restarting strategies of the Lanczos iteration were sought and implemented.

1. Orthogonality of Lanczos vectors

Reorthogonalization procedures require the knowledge of all previous Lanczos vectors that, in most cases, can be stored only on the hard disk. Careful choice and implementation of the reorthogonalization procedure are important to minimize the number of I/O operations. To quantify the level of orthogonality two terms can be defined.[53,55] Full orthogonality means that the dot product of different Lanczos vectors is not larger than the round-off error ε_u, whereas the term semiorthogonality is used if the dot product of different Lanczos vectors is not larger than $\sqrt{\varepsilon_u}$.

Full orthogonality among Lanczos vectors can be maintained by reorthogonalizing the new Lanczos vector against all previous ones in each Lanczos step. This brute-force procedure will be referred to as full reorthogonalization (FRO). Reorthogonalization is carried out in DEWE by using a numerically stable version of the Gram–Schmidt procedure (modified Gram–Schmidt procedure).[56]

It has been demonstrated that the requirement of full orthogonality can be alleviated and semiorthogonality of Lanczos vectors[53,55] is sufficient in order to compute accurate eigenpairs without extra or spurious levels entering the spectrum. The partial reorthogonalization (PRO) algorithm[53,55] implemented in DEWE is based on this observation. PRO uses a recurrence formula to estimate the current level of orthogonality among the Lanczos vectors without the explicit computation of their dot products. Our limited experience shows that for (ro)vibrational Hamiltonian matrices in DVR of size millions by millions, PRO is typically 55%–60% cheaper than FRO if 10–500 eigenpairs are to be computed. This gain is close to the gain 50% achievable with a so-called periodic reorthogonalization (PerRO) originally suggested by Grcar.[57] PerRO, which is based on a much simpler algorithm than PRO, reorthogonalizes every second Lanczos vector against all the previous ones. According to our extensive computations of 100–500 eigenpairs of matrices up to the size of $10^8 \times 10^8$, PerRO is a stable method providing accurate eigenvalues and eigenvectors without the introduction of spurious levels. The main advantage of PerRO over PRO is that it does not contain parameters to be optimized. Furthermore, PerRO is more robust against the round-off errors introduced by certain spectral transformation methods (e.g., CGM) tested, and it can be used in a black-box way also with restarted Lanczos iterations (see Sec. 2).

2. Restarted Lanczos algorithms

In general, it is not possible to predict the number of Lanczos iterations required to achieve convergence. Therefore, it is impossible to predict the storage requirements of the original procedure. Thus, to keep storage requirements under control the Lanczos algorithm must be occasionally restarted.

The thick-restart Lanczos method (TRLM)[55,58] was implemented in DEWE in order to compact the ever-growing Krylov subspace periodically. With an optimal choice of related parameters, the convergence rate of the Lanczos iteration is not worsened significantly. This algorithm was implemented and can be used in a nearly black-box way with the FRO and PerRO techniques.

An upper limit of the hard disk requirements can be defined for the restarted Lanczos procedures. This upper limit cannot be arbitrarily small. In principle, the number of Lanczos vectors stored must be at least as much as the number of eigenpairs to be computed. At the end of the computation, the Lanczos vectors can be replaced by the eigenvectors. In practice, in DEWE the minimal storage requirement (on the hard disk) for the computation of n_{eig} eigenvectors corresponds to the storage of $n_{\mathrm{eig}}+25$ Lanczos vectors, which is close to the optimal choice suggested also by other applications.[55,58,59]

Compared to the implicitly restarted Arnoldi algorithm available in ARPACK,[60] TRLM is more adequate for use in our variational rovibrational studies. First, it is specifically adapted for a symmetric eigenvalue problem; consequently it uses less arithmetic operations. Second, it is more tolerant to the loss of orthogonality of the vectors spanning the Krylov subspace. Further advantages of TRLM include that it can be restarted with any number of starting vectors and it retains a large part of the basis.

In order to use TRLM, the original Lanczos (OL) algorithm must be modified. Before restart, the Lanczos iteration runs according to the original algorithm given in Sec. II. After step m the Lanczos iteration is restarted, which assumes the following manipulations:[55,58]

(R1) Find all eigenvalues and eigenvectors of $\mathbf{T}_m$. The eigenvalues are the Ritz values.
(R2) Choose k Ritz values, $\lambda_1,\ldots,\lambda_k$, and the corresponding eigenvectors of $\mathbf{T}_m$, $\mathbf{y}_1,\ldots,\mathbf{y}_k$, to be saved in the restart procedure.
(R3) Let $\mathbf{Y}_k=[\mathbf{y}_1,\ldots,\mathbf{y}_k]$ and replace the first k columns of $\mathbf{Q}_m$ with $\mathbf{Q}_k\mathbf{Y}_k$, i.e., $\mathbf{Q}_k=\mathbf{Q}_k\mathbf{Y}_k$. The corresponding α_i and β_i values are replaced by $\alpha_i=\lambda_i$ and $\beta_i=\beta_m y_{mi}$, $i=1,2,\ldots,k$.
(R4) Set $\mathbf{q}_{k+1}=\mathbf{q}_{m+1}$.
(R5) FRO of $\mathbf{q}_{k+1}$ against $\mathbf{q}_i$, $i=1,2,\ldots,k$.
(R6) $\alpha_k=\mathbf{q}_k^T\mathbf{q}_{k+1}$.
(R7) $\mathbf{q}_{k+1}=\mathbf{q}_{k+1}-\alpha_k\mathbf{q}_k-\Sigma_{i=1}^{k}\beta_i\mathbf{q}_i$.
(R8) Continue the Lanczos iteration according to the original algorithm until the next restart, which repeats the steps (R1)–(R8) or until the convergence of the Lanczos iteration.

Note that $\mathbf{Q}_k\mathbf{Y}_k$ are the Ritz vectors. Due to step (R3), the projected matrix $\mathbf{T}_m$ is not tridiagonal in TRLM but has a special block structure. In this algorithm the production of Ritz vectors in step (R3) and the step (R7) is strongly I/O dependent. In these steps the vectors of the size of the Lanczos vectors are read from and written to the hard disk. The I/O operations can be minimized throughout these manipulations if the Lanczos vectors are stored on the hard disk in smaller blocks in direct access files. During the restart procedure the Ritz vectors are not produced one by one, but small blocks of all Ritz vectors are computed at once. In this way the Lanczos vectors are read from the disk, and the Ritz vectors are written to the disk only once during each restart. Furthermore, during the computation of Ritz vectors, the sum in (R7) is also evaluated, thus further saving I/O operations. The maximum size of the Krylov subspace is dynamically increased to the limiting value during the iteration, which also reduces the number of I/O operations. Due to the restarts, the Krylov subspace grows slower, and thus the cost of the reorthogonalization is also reduced compared to the nonrestarted version.

TABLE I. Memory requirement of DEWE: number of 64-bit reals stored in the main memory.

Part of DEWE	Quantity	No. of elements
Lanczos iteration	$\mathbf{x}$	$\mathcal{N}$
	$\mathbf{y}$	$\mathcal{N}$
Spectral transformation: SF (CGM)[a]	Scratch	$\mathcal{N}$ $(3\mathcal{N})$
$\mathbf{H}^{\mathrm{vib}}\mathbf{x}$	μ	$6\mathcal{N}$
	$\mathbf{U}+\mathbf{V}$	$\mathcal{N}$
	$(\mathbf{y}_x,\mathbf{y}_y,\mathbf{y}_z)$	$3\mathcal{N}$
Total		$13\mathcal{N}$ $(15\mathcal{N})$

[a]SF:shift-fold filter; CGM: conjugate gradient method.

C. Efficiency of the DEWE program

Memory requirements of the matrix-vector multiplication using different spectral transformation techniques and of the Lanczos iteration are collected in Table I. The memory requirement is $13\mathcal{N}$ (or $15\mathcal{N}$) depending on which spectral transformation technique is used. Lanczos vectors of size $\mathcal{N}$ are stored on the hard disk. In each reorthogonalization step the required Lanczos vectors are read from the hard disk. If a large number of eigenpairs is to be computed, the use of an efficient reorthogonalization technique together with a restarted Lanczos method is essential.

Figure 2 visualizes the timing of the Lanczos steps using different eigensolver techniques until the convergence of the lowest 100 eigenpairs is achieved for the $^{12}CH_4$ molecule. In this example the CGM method is used to carry out the spectral transformation, and its timing is given on curve (a) only for reference purposes. Curves (b) and (c) present the real timing, including also the spectral transformation (here CGM) part, of Lanczos iteration steps during the course of the Lanczos iteration if the thick-restart Lanczos algorithm (TRLM) with PerRO or the OL algorithm, without restart and with FRO is employed. Convergence is achieved after 654 and 662 steps using OL-FRO and TRLM-PerRO, respectively. Apparently, the number of Lanczos iterations re-

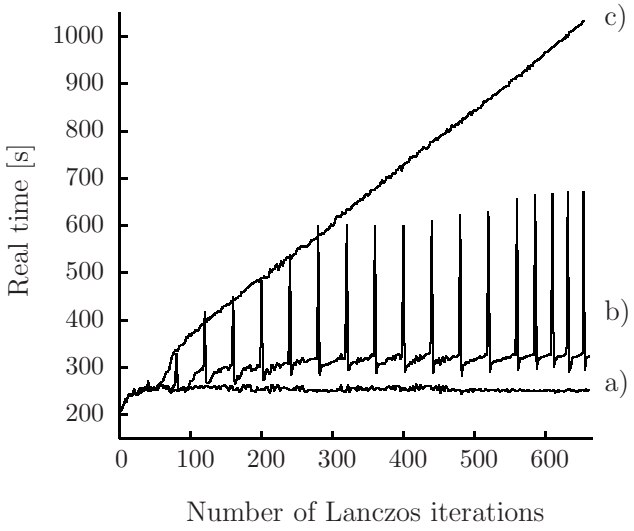

FIG. 2. Wall time in seconds of the average of two subsequent Lanczos steps during the course of the Lanczos iteration measured for (a) a single CGM spectral transformation step (plotted here only for reference). (b) A single Lanczos iteration step for the TRLM with PerRO (TRLM-PerRO). Maximally 155 eigenvectors were saved on the hard disk. The lowest 100 eigenvalues were converged after 662 Lanczos iteration steps. (c) A single Lanczos iteration step for the OL algorithm (without restart) with FRO (OL-FRO). The lowest 100 eigenvalues were converged after 654 Lanczos iteration steps. A detailed analysis of the curves is given in the text. Results are obtained for $^{12}CH_4$ using six grid points on each vibrational degree of freedom, which corresponds to a Hamiltonian matrix of size $10^7 \times 10^7$.

quired is only slightly increased in the case of thick-restart Lanczos with PerRO; however, the gain in real timing is enormous compared to the OL technique with FRO.

The timing of the spectral transformation part, curve (a) in Fig. 2, consists of matrix-vector multiplications that are CPU-intensive. As discussed in Sec. III, this part was parallelized with OPENMP. The differences between curves (b) and (a) or (c) and (a) in Fig. 2 originate from the reorthogonalization and the restarting parts. In these parts dot products of the Lanczos vectors are computed. The computation of dot products requires CPU usage but most importantly reading the Lanczos vectors from the hard disk, which is an I/O intensive part. Indeed, an enormous difference is experienced depending on how the Lanczos vectors are handled, as it can be observed by comparing curves (b) and (c) in Fig. 2.

If the Lanczos iteration is not restarted and full orthogonality is maintained among the Lanczos vectors, the real timing increases linearly with the number of Lanczos iteration steps. After 100 Lanczos iterations, the timing (mainly I/O operations) exceeds the time of the preconditioning step (parallelized with OPENMP using eight cores in this example). If the Lanczos iteration is restarted periodically, which corresponds to the peaks on curve (b), the Krylov subspace remains manageable throughout the Lanczos iteration. Note that between restarts the real timing increases approximately linearly, which corresponds to the increasing time required to maintain (semi)orthogonality among the increasing number of Lanczos vectors. The slope of the linear segments of curve (b) is approximately half of the slope of curve (c) in line with the fact that the average timing of PerRO is the half of that of FRO.

It is worth noting that if a less efficient but cheaper spectral transformation technique is employed, e.g., SF instead of CGM, the number of Lanczos iteration steps will be increased. In such a case, the usage of sophisticated reorthogonalization and restarting techniques, such as those presented here, is essential.

According to our experience, if a large number of eigenpairs are to be computed, it is useful to replace the CGM with the SF spectral transformation technique. This preference is explained as follows. The SF and CGM filters require 2 and 30–50 matrix-vector multiplications in each Lanczos step, respectively. Although the SF filter produces a matrix with less optimal spectral properties than CGM, it typically requires three to five times as many Lanczos iterations than CGM. The total number of matrix-vector multiplication during the course of the whole Lanczos procedure with the SF filter requires five to ten times less matrix-vector multiplications than with CGM. This gain of a factor of five to ten in the CPU usage can be exploited only if the presented reorthogonalization and restarting techniques are employed. Otherwise, this gain of CPU time is lost due to the increased time of the increased number of I/O operations.

V. NUMERICAL RESULTS ON METHANE

An optimal combination of the Watson Hamiltonian, the Hermite-DVR, and the sophisticated matrix-vector multiplication and eigensolver techniques presented in this paper allows the computation of hundreds of numerically exact eigenpairs of arbitrary semirigid five-atomic molecules on a nowadays standard server machine. Until now such a goal was only achievable by using tailor-made Hamiltonians with contracted basis sets and by exploiting symmetry of the molecules investigated.[12,11,61] Our approach is computationally feasible for five-atomic systems even if the molecule studied has no symmetry or if it is not exploited. For symmetrical molecules the computational requirements can be further reduced, but this was not done during this preliminary application on methane.

Due to the lack of a detailed experimental line-list of methane and its isotopologues, there have been several attempts to develop algorithms allowing the computation of a large number of accurate eigenpairs at higher-energy regions. These studies include nonvariational attempts, such as that of Wang and Sibert,[62] Duncan and Law,[63] and Halonen and co-workers.[64,65] As to variational ones, Xie and Tennyson[66,67] solved the stretching and bending subproblems of a molecule of XY_4 composition. Carter *et al.*[68,69] computed variationally the rovibrational energy levels of CH_4, CH_3D, CH_2D_2, CHD_3, and CD_4 using the MULTIMODE program using an approximate kinetic energy operator and the original and an adjusted forms of the quartic force field of Lee *et al.*[70] Chakraborty *et al.*[71] computed the rovibrational energy levels of CH_4 for $J=0-50$ using MULTIMODE using an approximate kinetic energy operator.

As to sophisticated PESs of methane, Marquardt and Quack[72,73] constructed a global analytic PES of the electronic ground state of methane by fitting a flexible and robust model potential to lower-level *ab initio* energies and adjusting this fit empirically to experimental observables.

TABLE II. Convergence properties of the DEWE approach: ZPVE and vibrational fundamentals of $^{12}CH_4$, in cm^{-1}, obtained with the T8 force field (Ref. 74).

Label	Conv.[a,b]	(3,3)[a,c]			(4,4)[a,c]			(5,5)[a,c]		
$(00)(00)A_1$	9691.5	9684.2		[7.4]	9690.9		[0.6]	9691.5		[0.1]
$(00)(01)F_2$	1311.7	1307.6	{2.4}	[4.1]	1310.6	{0.3}	[1.1]	1311.7	{0.0}	[0.0]
$(00)(10)E$	1533.2	1533.0	{0.9}	[0.3]	1532.6	{0.1}	[0.7]	1533.2	{0.0}	[0.0]
$(10)(00)A_1$	2913.8	-[d]		-[d]	2922.9		[−9.2]	2910.5		[3.3]
$(01)(00)F_2$	3013.6	3010.8	{4.0}	[2.8]	2999.3	{0.0}	[14.3]	3013.5	{0.1}	[0.1]

[a]Results obtained with DEWE using a (n_b,n_s) direct-product grid. n_b and n_s, referred to as (n_b,n_s), grid points were used for the bending- and stretching-type vibrational degrees of freedom, resulting in a direct-product grid of size $n_b^5 n_s^4$. Nuclear masses, $m_C=11.996\ 709$ u and $m_H=1.007\ 276$ u were employed. The reference structure was a tetrahedron with the carbon in the center and hydrogens on the apices with $r(CH)=1.0890$ Å. The actual values of **c** and **l** matrices employed are given in the supplementary material.
[b]Converged results obtained with DEWE.
[c]Maximum splittings of degenerate levels due to the incomplete convergence are given in braces as $\{\nu(\text{highest})-\nu(\text{lowest})\}$. Deviations of energy levels from converged results are given in brackets, $[\nu(\text{Conv.})-\nu(n_b,n_s)]$.
[d]Deviation from the converged result is larger than 20 cm^{-1}.

Schwenke and Partridge[74,75] computed an eighth-order force field, called T8, of methane and computed vibrational energy levels using a tailor-made variational program developed for this molecule. The published variational vibrational energy levels were converged to about 15 cm^{-1}.

Oyanagi *et al.*[76] developed full-dimensional *ab initio* potential energy and DMSs using the modified Shepard interpolation method based on a fourth order Taylor expansion. The generated surface was used with MULTIMODE using an approximate kinetic energy operator to compute vibrational band origins (VBOs) and vibrational intensities of methane.

Wang and Carrington[11] developed a variational computer code for the computation of rovibrational energy levels of methane employing an internal coordinate Hamiltonian, a two-stage contraction technique, and iterative eigensolver methods. At about the same time, Yu[12] also developed a similar tailor-made variational code for methane.

Throughout this work the T8 force field[74] was employed because this force field was used previously with tailor-made variational programs for $^{12}CH_4$.[11,12,61] Completely new VBOs are given here for the $^{12}CH_2D_2$ isotopologue.

To obtain the results described below, the reference structure **c** was chosen as the minimum of the T8 PES. The **l** matrix was constructed by carrying out a harmonic analysis with the diagonal-only force-constants in Ref. 70. The actual values of **c** and **l** used are provided in the supplementary material. As the DEWE approach is numerically exact, the actual values of **c** and **l**, satisfying the conditions given in Eq. (2), affect only the convergence rate but do not influence the values of the converged eigenpairs. This is in line with the simple physical fact that the choice of **c** and **l** is merely a possible choice of coordinates. It is worth noting that degenerate levels converge fast enough only if the corresponding symmetry of the molecule is accurately reflected by the numerical values of **c** and **l**.

In the kinetic energy part the nuclear masses $m_C=11.996\ 709$ u, $m_D=2.013\ 553$ u, and $m_H=1.007\ 276$ u were employed. The Radau coordinates employed in the T8 PES were computed using the nuclear masses of the parent isotopologue for either $^{12}CH_4$ or $^{12}CH_2D_2$.

A. CH_4

The convergence properties of the DEWE approach are demonstrated by the results given in Table II, where the fundamentals of $^{12}CH_4$ obtained with small direct-product grids are compared with the converged results. In the notation (n_b,n_s) used henceforth, n_b and n_s correspond to the number of grid points used for each bending- and stretching-type vibrational degree of freedom and to a direct-product grid of size $n_b^5 n_s^4$. The accuracy of the zero-point vibrational energy (ZPVE) is remarkable already with a (3,3) grid (total size of 19 683), and it is converged to better than 1 cm^{-1} using a (4,4) grid (total size of 262 144). Using a (5,5) grid (total size of 1 953 125) the ZPVE and the fundamentals, except $(10)(00)A_1$, are converged to better than 0.1 cm^{-1}. This behavior contradicts somewhat the traditional view that DVR requires the usage of a relatively large number of quadrature points. The symmetry labels of the VBOs follows the polyad notation $(v_1v_3)(v_2v_4)$.

The timing and storage requirements of the computation of 20 eigenvalues and eigenvectors on a (5,5) grid are as follows. The size of a single Lanczos vector is 15 MB; thus 194 and 745 MB were the total memory and hard disk requirements, respectively. On a nowadays standard server machine, such a computation lasts 20–30 minutes.

The lowest 96 energy levels (degeneracy not counted), up to ~6125 cm^{-1}, of $^{12}CH_4$ obtained with DEWE and a (9,8) grid are presented in Table III. The changes in the vibrational energies upon the increase in the size of the direct-product grid from (8,7) to (9,8) are also given in the table, which allows to estimate the level of convergence. Most of the levels are most likely converged to better than 0.05 cm^{-1} already with a grid (8,7). The change in the $(20)(00)A_1$ level was the largest, 1.37 cm^{-1}, in this range upon the increase in the basis size from (8,7) to (9,8).

Note that the symmetry labels corresponding to the VBOs at 5619.44 and 5624.75 cm^{-1} were given incorrectly in all previously published tables.[11,12,61] The correct assignment is $(00)(22)E$ and $(01)(02)F_1$ for the lower and upper levels, respectively.

The timing and storage requirements corresponding to the results presented in Table III corresponding to a (9,8) grid (total size of 241 864 704) [(8,7) grid (total size of 78 675 968)] and 100 eigenpairs are as follows. The size of a single Lanczos vector is 1.8 GB [0.59 GB]; thus 23.4 GB [7.6 GB] memory is used, and 464 GB [152 GB] data are stored on the hard disk. On a nowadays standard server ma-

TABLE III. ZPVE and VBOs of $^{12}CH_4$, in cm^{-1}, obtained with DEWE and the T8 force field (Ref. 74).

Label[a]	DEWE[b]	δ[c]	Δ_C[d]	Δ_E[e]
$(00)(00)A_1$	9691.54	0.00	−0.01	–
$(00)(01)F_2$	1311.74	0.00	0.00	−0.98
$(00)(10)E$	1533.25	0.00	−0.01	0.08
$(00)(02)A_1$	2589.77	0.00	0.00	−2.73
$(00)(02)F_2$	2616.23	0.00	0.01	−1.97
$(00)(02)E$	2627.29	0.00	0.00	−2.67
$(00)(11)F_2$	2831.52	0.00	0.00	−1.20
$(00)(11)F_1$	2846.90	0.00	0.01	−0.82
$(10)(00)A_1$	2913.71	−0.05	0.00	2.77
$(01)(00)F_2$	3013.60	0.00	0.00	5.89
$(00)(20)A_1$	3063.48	0.00	0.00	0.17
$(00)(20)E$	3065.00	0.00	0.01	0.14
$(00)(03)F_2$	3874.69	0.00	0.05	−4.20
$(00)(03)A_1$	3912.22	0.00	0.04	−3.03
$(00)(03)F_1$	3924.04	0.00	0.04	−3.52
$(00)(03)F_2$	3935.30	0.00	0.02	−4.38
$(00)(12)E$	4104.38	0.00	0.06	0.24
$(00)(12)F_1$	4131.22	0.00	0.04	−2.49
$(00)(12)A_1$	4135.72	0.00	0.04	−2.70
$(00)(12)F_2$	4144.81	0.00	0.02	−1.95
$(00)(12)E$	4153.70	0.00	0.02	−2.70
$(00)(12)A_2$	4164.30	0.00	0.02	−2.39
$(10)(01)F_2$	4221.84	−0.05	0.00	1.62
$(01)(01)F_2$	4314.22	0.00	0.01	4.99
$(01)(01)E$	4317.58	0.00	0.01	4.62
$(01)(01)F_1$	4317.82	0.00	0.01	4.76
$(01)(01)A_1$	4318.41	0.01	0.01	4.28
$(00)(21)F_2$	4350.02	0.00	0.05	−1.31
$(00)(21)F_1$	4364.68	0.00	0.03	−1.09
$(00)(21)F_2$	4379.71	0.00	0.02	−0.73
$(10)(10)E$	4432.22	−0.05	0.00	2.90
$(01)(10)F_1$	4531.36	0.00	0.01	6.19
$(01)(10)F_2$	4537.81	0.00	0.01	5.95
$(00)(30)E$	4591.88	0.01	0.04	0.13
$(00)(30)A_2$	4595.13	0.00	0.03	0.15
$(00)(30)A_1$	4595.40	0.00	0.03	0.06
$(00)(04)A_1$	5128.02	0.11	0.27	−6.68
$(00)(04)F_2$	5148.96	0.04	0.24	−5.72
$(00)(04)E$	5173.81	0.05	0.20	−6.65
$(00)(04)F_2$	5215.52	0.03	0.16	−4.23
$(00)(04)E$	5234.63	0.03	0.13	−5.72
$(00)(04)F_1$	5236.32	0.03	0.13	−5.54
$(00)(04)A_1$	5247.02	0.04	0.13	−7.04
$(00)(13)F_2$	5375.41	0.01	0.25	1.54
$(00)(13)F_1$	5393.98	0.00	0.23	−0.29
$(00)(13)E$	5428.38	0.00	0.18	−3.72
$(00)(13)F_2$	5434.05	0.01	0.17	−4.47
$(00)(13)F_1$	5441.27	0.00	0.15	−4.48
$(00)(13)F_1$	5467.01	0.00	0.12	−4.09
$(10)(02)A_1$	5492.95	0.17	−0.01	−6.51
$(00)(13)F_2$	5448.36	0.00	0.13	−3.24
$(10)(02)F_2$	5520.91	−0.04	0.01	−3.74
$(10)(02)E$	5533.66	−0.03	0.02	−1.48
$(01)(02)F_2$	5584.97	0.00	0.02	3.01
$(01)(02)A_1$	5602.82	0.04	0.06	3.50
$(01)(02)F_2$	5611.76	0.01	0.03	11.25
$(01)(02)F_1$	5612.09	0.00	0.02	5.90
$(01)(02)E$	5612.65	0.01	0.06	12.63
$(00)(22)A_1$	5614.19	0.01	0.29	2.23
$(00)(22)E$	5619.44	0.01	0.25	12.66
$(01)(02)F_2$	5623.03	0.00	0.02	5.37
$(01)(02)F_1$	5624.75	0.01	0.03	−6.48
$(00)(22)F_2$	5645.08	0.00	0.23	−4.42
$(00)(22)E$	5657.05	0.00	0.14	−3.45
$(00)(22)F_1$	5658.21	0.00	0.16	−2.91
$(00)(22)A_2$	5666.50	0.00	0.11	−4.14
$(00)(22)F_2$	5670.62	0.00	0.13	−1.64
$(00)(22)A_1$	5683.98	0.00	0.20	−1.54
$(00)(22)E$	5693.41	0.00	0.11	−1.99
$(10)(11)F_2$	5725.07	−0.05	0.05	4.61
$(10)(11)F_1$	5743.02	−0.05	0.04	13.03
$(20)(00)A_1$	5782.40	1.37	−0.22	7.85
$(01)(11)F_2$	5816.74	−0.01	0.02	9.91
$(01)(11)F_1$	5820.35	0.00	0.01	6.94
$(01)(11)E$	5827.80	0.07	0.04	9.24
$(01)(11)A_1$	5830.24	0.18	0.01	1.16
$(01)(11)E$	5837.90	0.01	0.02	3.18
$(01)(11)A_2$	5837.98	0.00	0.02	−6.09
$(01)(11)F_2$	5838.95	0.00	0.02	10.35
$(01)(11)F_1$	5842.15	0.00	0.02	3.74
$(11)(00)F_2$	5853.52	−0.09	0.07	−33.80
$(00)(31)F_2$	5867.40	0.00	0.77	0.26
$(00)(31)F_1$	5880.94	0.00	0.67	−1.92
$(00)(31)F_2$	5895.37	0.00	0.70	−1.25
$(00)(31)F_1$	5909.90	0.00	0.72	−0.19
$(10)(20)A_1$	5932.90	0.23	0.13	38.62
$(10)(20)E$	5949.38	−0.05	0.18	25.21
$(02)(00)A_1$	5960.68	0.25	0.14	7.41
$(02)(00)F_2$	5993.41	−0.02	0.05	11.28
$(02)(00)E$	6031.83	0.54	0.02	12.04
$(01)(20)F_2$	6047.93	−0.01	0.04	6.71
$(01)(20)F_1$	6054.40	0.00	0.05	4.90
$(01)(20)F_2$	6059.47	−0.01	0.09	5.85
$(00)(40)A_1$	6116.58	0.46	2.93	0.17
$(00)(40)E$	6118.43	0.03	2.77	0.19
$(00)(40)E$	6124.01	0.03	2.51	0.16

[a]Energy levels are labeled as $(v_1v_3)(v_2v_4)$, following the polyad notation of Carrington *et al.* (Refs. 11 and 61).

[b]Results obtained with the DEWE program. Nuclear masses, $m_C = 11.996\,709$ u and $m_H = 1.007\,276$ u were used. The reference structure was a tetrahedron with the carbon in the center and hydrogens on the apices with $r(CH) = 1.0890$ Å. The actual values of the **c** and **I** matrices employed are given in the supplementary material. 9 and 8, referred to as (9,8), grid points were used for the bending- and stretching-type vibrational degrees of freedom, resulting in a direct-product grid of total size of 241 864 704.

[c]Deviations of vibrational energy levels obtained with (9,8) and (8,7) grid points, $\delta = \tilde{\nu}(\text{DEWE}(9,8)) - \tilde{\nu}(\text{DEWE}(8,7))$.

[d]Deviations of vibrational energy levels obtained with DEWE(9,8) from results of Carrington *et al.* (Refs. 11 and 61), $\Delta_C = \tilde{\nu}$ (Ref. 61) $- \tilde{\nu}(\text{DEWE}(9,8))$.

[e]Deviations of vibrational energy levels obtained with DEWE(9,8) and vibrational band origins extracted from experimental data (Refs. 78–80), $\Delta_E = \tilde{\nu}(\text{Exp}) - \tilde{\nu}(\text{DEWE}(9,8))$.

chine, the computation lasts ~5 months [~2 months], depending on the processor and the disk capacities.

B. CH_2D_2

In order to supplement this study with completely new numerical results, the first 40 well-converged vibrational en-

TABLE IV. ZPVE and VBOs of $^{12}CH_2D_2$, in cm^{-1}, obtained with DEWE and the T8 force field (Ref. 74).

Label[a]		DEWE[b]	δ [c]	Δ_E [d]
ZPVE	A_1	8432.21	0.01	–
ν_4	A_1	1033.11	0.00	−0.06
ν_7	B_1	1091.54	0.00	−0.35
ν_9	B_2	1236.90	0.00	−0.62
ν_5	A_2	1331.23	0.00	0.18
ν_3	A_1	1435.27	0.00	−0.14
$2\nu_4$	A_1	2054.51	−0.01	−0.35
$\nu_4+\nu_7$	B_1	2125.13	0.00	−0.45
ν_2	A_1	2144.29	−0.05	1.40
$2\nu_7$	A_1	2202.31	−0.04	0.91
ν_8	B_2	2231.83	−0.01	2.86
$\nu_4+\nu_9$	B_2	2284.55	0.00	1.43
$\nu_7+\nu_9$	A_2	2331.28	0.00	−1.58
$\nu_4+\nu_5$	A_2	2364.85	0.00	
$\nu_5+\nu_7$	B_2	2422.44	0.00	−0.41
$2\nu_9$	A_1	2460.04	−0.01	−1.24
$\nu_3+\nu_4$	A_1	2470.07	0.00	−0.87
$\nu_3+\nu_7$	B_1	2516.53	0.00	−1.08
$\nu_5+\nu_9$	B_1	2561.19	0.00	−0.64
$2\nu_5$	A_1	2658.05	0.00	0.29
$\nu_3+\nu_9$	B_2	2672.46	0.00	−0.77
$\nu_3+\nu_5$	A_2	2765.98	0.00	
$2\nu_3$	A_1	2856.07	−0.02	−0.40
ν_1	A_1	2970.98	−0.21	5.50
ν_6	B_1	3006.09	−0.04	6.17
$3\nu_4$	A_1	3066.96	−0.02	
$2\nu_4+\nu_7$	B_1	3142.32	−0.01	
$\nu_2+\nu_4$	A_1	3182.58	−0.03	
$\nu_4+2\nu_7$	A_1	3209.95	−0.03	
$\nu_2+\nu_7$	B_1	3233.07	−0.03	
$\nu_4+\nu_8$	B_2	3241.24	−0.01	
$3\nu_7$	B_1	3306.23	−0.04	
$2\nu_4+\nu_9$	B_2	3312.08	−0.01	
$\nu_7+\nu_8$	A_2	3319.38	−0.01	
$\nu_4+\nu_7+\nu_9$	A_2	3375.92	0.00	
$\nu_2+\nu_9$	B_2	3380.77	−0.05	
$2\nu_4+\nu_5$	A_2	3386.52	−0.01	
$2\nu_7+\nu_9$	B_2	3440.30	−0.03	
$\nu_4+\nu_5+\nu_7$	B_2	3447.78	0.00	
$\nu_8+\nu_9$	A_1	3456.42	0.00	

[a]Assignment of vibrational energy levels follows that of Ref. 80.
[b]Results obtained with the DEWE program. Nuclear masses m_C = 11.996 709 u, m_D = 2.013 553 u, and m_H = 1.007 276 u were used. The reference structure was a tetrahedron with the carbon in the center and hydrogens on the apices with $r(CH)=r(CD)=1.0890$ Å were used. The actual values of **c** and **l** matrices employed are given in the supplementary material. Grid points 10 and 8, referred to as (10,8), were used for the bending- and stretching-type vibrational degrees of freedom, resulting in a direct-product grid of a total size of 409 600 000.
[c]Deviation of vibrational energy levels obtained by using the DEWE program and the (10,8) and (9,7) grids, $\delta=\tilde{\nu}(\text{DEWE}(10,8))-\tilde{\nu}(\text{DEWE}(9,7))$.
[d]Deviation of computed levels from experimental data, $\Delta_E=\tilde{\nu}$ (Ref. 80) $-\tilde{\nu}(\text{DEWE}(10,8))$. Δ_E is given where experimental data were available.

ergy levels of $^{12}CH_2D_2$ were computed. For this isotopologue of methane, these are the first numerically exact results, i.e., without introducing any approximations in the variational vibrational treatment.

In Table IV the ZPVE and the first 39 VBOs referenced to the ZPVE are presented for $^{12}CH_2D_2$ up to ~3500 cm^{-1}. Most of the energy levels obtained from the largest computation using a (10,8) grid are most likely converged within 0.01 cm^{-1}. In Table IV the deviations of the energy levels obtained with the (10,8) and (9,7) grids are given, which are typically less than 0.05 cm^{-1}. There is a single level that does not fit in this threshold located at 2970.98 cm^{-1}. It changes by –0.21 cm^{-1} upon the increase in the basis to (10,8) from (9,7). Based on the available experimental data, this level was assigned to $\nu_1 A_1$.

The timing and storage requirements corresponding to the results presented in Table IV, corresponding to a (10,8) grid (total size of 409 600 000) and 40 eigenvalues are as follows. The size of a single Lanczos vector is 3.1 GB; thus 40 GB memory is used by DEWE, and 214 GB data are stored on the hard disk. On a nowadays standard server machine, the computation lasts 6–8 weeks.

VI. CONCLUSIONS AND OUTLOOK

Efficiency considerations of an algorithm and computer code, called DEWE,[29] using the Hermite-DVR of the Watson Hamiltonian coupled with Lanczos-type iterative eigensolvers were presented in detail. Due to the universal form of the Watson Hamiltonian,[16] the DEWE protocol can be used to compute eigenpairs of semirigid molecules with arbitrary bonding arrangements without the introduction of any kind of numerical approximation. The limitation of the DEWE program is introduced by the properties of the internal coordinates and the body-fixed frame used to express the vibrational Hamiltonian. The use of rectilinear internal coordinates and the Eckart body-fixed frame favoring the neighborhood of the chosen reference structure makes the approaches based on the Watson Hamiltonian inefficient for the description of molecules having large amplitude internal motions. However, for the description of the nuclear motions of semirigid molecules with a single minimum, the Watson Hamiltonian is an excellent choice.

In spite of the fact that DEWE uses a direct-product DVR grid, the ideal combination of the Hermite polynomials used to construct the DVR and the rectilinear internal coordinates used to express the vibrational Hamiltonian allow the computation of hundreds of numerically exact eigenvalues and eigenfunctions of molecules of up to five nuclei using sophisticated eigensolvers on nowadays standard server machines.

An efficient matrix-vector multiplication scheme specifically developed for the Watson Hamiltonian is presented. The matrix-vector multiplication is the most CPU-intensive part of variational computations using a direct-product grid with an iterative eigensolver, apart from some cases when a very large number of eigenpairs for small systems are to be computed. Therefore, an algorithm parallelized with OPENMP (Ref. 37) was developed.

The actual choice of the spectral transformation method and the handling of the spread of round-off errors are rather delicate problems, which were addressed in this work. Advantages and drawbacks of simple polynomial transforma-

tion techniques, exponential filters using a Chebyshev expansion, and shift-invert techniques using the conjugate gradient method were investigated.

In order to compute not only eigenvalues but also eigenvectors, the Lanczos vectors must be stored on the hard disk. To avoid the computation of extra copies of exact levels or spurious eigenvalues, the Lanczos vectors need to be reorthogonalized. In order to minimize the I/O operations required for reading the previous Lanczos vectors, it seems to be enough to maintain semiorthogonality using PerRO.[57]

To keep manageable the size of the Krylov subspace spanned by the Lanczos vectors, it seems best to restart the Lanczos iteration periodically using the thick-restart Lanczos algorithm.[55] This algorithm performs particularly well, as it was developed specifically for real symmetric matrices. According to our experience in the computation of vibrational eigenpairs, restarting the Lanczos iteration does not significantly worsen the convergence rate.

In a nutshell, there are three main factors that contribute to the total timing of the DEWE approach: (a) the number of matrix-vector multiplications in a single Lanczos step, which is a CPU-intensive step; (b) reorthogonalization of the Lanczos vectors to maintain the (semi)orthogonality among them, which is an I/O intensive step and CPU usage becomes significant only if the size of the Krylov subspace is very large; and (c) the convergence rate of the total Lanczos iteration. After having studied the interplay of these three factors in considerable detail, we found that for larger applications, specifically for the computation of the lowest few hundred eigenpairs of five-atomic molecules, a simple and clever choice is the usage of the shift-fold filter, periodic reorthogonalization, and the thick-restart Lanczos algorithm.

When not the lowest eigenvalues but an interior part of the spectrum is to be computed, the shift-invert technique seems to be an appealing choice, but to find an efficient black-box method to carry out the spectral transformation is challenging. A safe and practical technique might be the usage of a carefully optimized shifted version of the exponential transformation, the shift-Gaussian filter.

The computation of interior eigenvalues opens a promising route toward the computation of a very large number of eigenvalues and eigenvectors, i.e., toward the determination of the complete spectrum. This task could be distributed to practically independent computing nodes by distributing smaller ranges of the spectrum to different machines. This would make the computation of a very large number of eigenpairs an embarrassingly parallel problem. Eigenpairs from different ranges of the spectrum can be converged independently, i.e., the lower end of the spectrum could be computed using a smaller grid. If only very few interior eigenvalues, e.g., ten eigenvalues, are required in each run, the total storage requirement, Lanczos and a few auxiliary vectors, of the computation fits into the main memory of nowadays standard machines, which eliminates the time-consuming I/O operations on the hard disk.

The DEWE algorithm can be further improved if symmetry properties are exploited for the computation of eigenpairs of symmetric species. The symmetry-adapted Lanczos algorithm suggested by Wang and Carrington[77] can be straightforwardly adapted to our approach to compute levels corresponding to different irreducible representations of Abelian groups in separate runs. As normal coordinates, a special case of Watson's rectilinear internal coordinates, correspond to irreducible representations of the point group of the molecule, the storage requirements of Lanczos and auxiliary vectors might be reduced accordingly. This modification is also extremely useful to increase the convergence rate of the Lanczos iteration.

The DEWE algorithm and computer code were used to compute the eigenpairs of the $^{12}CH_4$ and $^{12}CH_2D_2$ isotopologues of the methane molecule. The VBOs of $^{12}CH_4$ provide a good validation for the DEWE approach as variational results are available in the literature[11,12,61] using the same PES but different algorithms. The convergence of the energy levels obtained with these programs specifically developed for $^{12}CH_4$ was achieved and exceeded by our DEWE approach, which can be employed not only for $^{12}CH_4$ but also for other semirigid molecules. To the best of our knowledge, this study presented the first benchmark variational results for the $^{12}CH_2D_2$ isotopologue using the T8 PES.

ACKNOWLEDGMENTS

The research performed in Budapest was mainly supported by the Hungarian Scientific Research Fund (Grant No. OTKA K72885). A.G.C. and J.S. are thankful for additional support received through the EU FP6 QUASAAR Program. J.S. also acknowledges the support through the Centers of Excellence Program of the Slovak Academy of Sciences (COMCHEM) (Contract No. II/1/2007).

[1] J. Quant. Spectrosc. Radiat. Transf. **110**, 9–10, pp. 531–782 (2009), HITRAN Special Issue.
[2] J. Tennyson, P. F. Bernath, L. R. Brown, A. Campargue, M. R. Carleer, A. G. Császár, R. R. Gamache, J. T. Hodges, A. Jenouvrier, O. V. Naumenko, O. L. Polyansky, L. S. Rothman, R. A. Toth, A. C. Vandaele, N. F. Zobov, L. Daumont, A. Z. Fazliev, T. Furtenbacher, I. E. Gordon, S. N. Mikhailenko, and S. V. Shirin, J. Quant. Spectrosc. Radiat. Transf. **110**, 573 (2009).
[3] O. L. Polyansky, A. G. Császár, S. V. Shirin, N. F. Zobov, P. Barletta, J. Tennyson, D. W. Schwenke, and P. J. Knowles, Science **299**, 539 (2003).
[4] P. Barletta, S. V. Shirin, N. F. Zobov, O. L. Polyansky, J. Tennyson, E. F. Valeev, and A. G. Császár, J. Chem. Phys. **125**, 204307 (2006).
[5] L. Lodi, R. N. Tolchenov, J. Tennyson, A. E. Lynas-Gray, S. V. Shirin, N. F. Zobov, O. L. Polyansky, A. G. Császár, J. N. P. van Stralen, and L. Visscher, J. Chem. Phys. **128**, 044304 (2008).
[6] M. J. Bramley and T. Carrington, Jr., J. Chem. Phys. **99**, 8519 (1993).
[7] G. Czakó, T. Furtenbacher, A. G. Császár, and V. Szalay, Mol. Phys. **102**, 2411 (2004).
[8] T. Furtenbacher, G. Czakó, B. T. Sutcliffe, A. G. Császár, and V. Szalay, J. Mol. Struct. **780–781**, 283 (2006).
[9] J. Tennyson, M. A. Kostin, P. Barletta, G. J. Harris, O. L. Polyansky, and N. F. Zobov, Comput. Phys. Commun. **163**, 85 (2004).
[10] I. N. Kozin, M. M. Law, J. Tennyson, and J. M. Hutson, Comput. Phys. Commun. **163**, 117 (2004).
[11] X.-G. Wang and T. Carrington, Jr., J. Chem. Phys. **119**, 101 (2003).
[12] H.-G. Yu, J. Chem. Phys. **121**, 6334 (2004).
[13] H.-G. Yu, J. Chem. Phys. **120**, 2270 (2004).
[14] X.-G. Wang and T. Carrington, Jr., J. Chem. Phys. **129**, 234102 (2008).
[15] M. Mladenović, J. Chem. Phys. **112**, 1070 (2000).
[16] J. K. G. Watson, Mol. Phys. **15**, 479 (1968).
[17] C. Eckart, Phys. Rev. **47**, 552 (1935).
[18] The name "Watson Hamiltonian" has been widely used during the past decades in molecular spectroscopy. Following common practice, this name is used also in this work. We feel, however, that it is more appropriate to call this Hamiltonian the Eckart–Watson Hamiltonian. This way

one refers both to Eckart's choice of the body-fixed frame and Watson's contributions by choosing orthogonal rectilinear internal coordinates and simplifying the quantum Hamiltonian to its well-known compact form. The term Eckart–Watson Hamiltonian has been used, for example, in Refs. 19, 20, 24, and 29.
[19] B. T. Sutcliffe, Adv. Chem. Phys. **114**, 1 (2000).
[20] B. T. Sutcliffe, *Molecular Hamiltonians*, in Handbook of Molecular Physics and Quantum Chemistry, Vol. 1, edited by S. Wilson (Wiley, Chichester, 2003), Chap. 32, pp. 501–525.
[21] K. M. Dunn, J. E. Boggs, and P. Pulay, J. Chem. Phys. **85**, 5838 (1986).
[22] K. M. Dunn, J. E. Boggs, and P. Pulay, J. Chem. Phys. **86**, 5088 (1987).
[23] T. Seideman and W. H. Miller, J. Chem. Phys. **97**, 2499 (1992).
[24] F. Wang, F. R. W. McCourt, and E. I. von Nagy-Felsobuki, Chem. Phys. Lett. **269**, 138 (1997).
[25] J. M. Bowman, S. Carter, and X. C. Huang, Int. Rev. Phys. Chem. **22**, 533 (2003).
[26] T. Yonehara, T. Yamamoto, and S. Kato, Chem. Phys. Lett. **393**, 98 (2004).
[27] G. Rauhut, J. Chem. Phys. **121**, 9313 (2004).
[28] O. Christiansen, Phys. Chem. Chem. Phys. **9**, 2942 (2007).
[29] E. Mátyus, G. Czakó, B. T. Sutcliffe, and A. G. Császár, J. Chem. Phys. **127**, 084102 (2007).
[30] D. Luckhaus, J. Chem. Phys. **113**, 1329 (2000).
[31] D. Lauvergnat and A. Nauts, J. Chem. Phys. **116**, 8560 (2002).
[32] S. N. Yurchenko, W. Thiel, and P. Jensen, J. Mol. Spectrosc. **245**, 126 (2007).
[33] E. Mátyus, G. Czakó, and A. G. Császár, J. Chem. Phys. **130**, 134112 (2009).
[34] C. Lanczos, J. Res. Natl. Bur. Stand. **45**, 255 (1950).
[35] J. K. Cullum and R. A. Willoughby, *Lanczos Algorithms for Large Symmetric Eigenvalue Computations* (Birkhauser, Boston, 1985).
[36] Y. Saad, *Iterative Methods for Sparse Linear Systems* (Society for Industrial and Applied Mathematics, Philadelphia, PA, 2003).
[37] www.openmp.org provides specification for OpenMP Application Program Interface, which supports multi-platform shared-memory parallel programming in C/C++ and Fortran.
[38] See EPAPS supplementary material at http://dx.doi.org/10.1063/1.3187528 for the definition of normal coordinates used in this study and further discussion on the parallel speed-up of the matrix-vector multiplication as well as on the relative separation of eigenvalues after the spectral transformation techniques studied here.
[39] H.-G. Yu and G. Nyman, Chem. Phys. Lett. **298**, 27 (1998).
[40] T. Ericsson and A. Ruhe, Math. Comput. **35**, 1251 (1980).
[41] H. Kono, Chem. Phys. Lett. **214**, 137 (1993).
[42] R. E. Wyatt, Phys. Rev. E **51**, 3643 (1995).
[43] L.-W. Wang and A. Zunger, J. Chem. Phys. **100**, 2394 (1994).
[44] I. J. Farkas, I. Derényi, A.-L. Barabási, and T. Vicsek, Phys. Rev. E **64**, 026704 (2001).
[45] H.-G. Yu and G. Nyman, J. Chem. Phys. **110**, 7233 (1999).
[46] H.-G. Yu, J. Chem. Phys. **114**, 2967 (2001).
[47] H. Tal-Ezer and R. Kosloff, J. Chem. Phys. **81**, 3967 (1984).
[48] M. C. Payne, M. P. Teter, D. C. Allan, T. A. Arias, and J. D. Joannopoulos, Rev. Mod. Phys. **64**, 1045 (1992).
[49] S.-W. Huang and T. Carrington, Jr., J. Chem. Phys. **112**, 8765 (2000).
[50] B. Poirier and T. Carrington, Jr., J. Chem. Phys. **114**, 9254 (2001).
[51] B. Poirier and T. Carrington, Jr., J. Chem. Phys. **116**, 1215 (2002).
[52] S. Tomov, J. Langou, J. Dongarra, A. Canning, and L.-W. Wang, International Journal of Computational Science and Engineering **2**, 205 (2006).
[53] H. D. Simon, Math. Comput. **42**, 115 (1984).
[54] X.-G. Wang and T. Carrington, Jr., J. Chem. Phys. **117**, 6923 (2002).
[55] K. Wu and H. D. Simon, Lawrence Berkeley National Laboratory Report No. 41412, 1998.
[56] G. H. Golub and C. F. V. Loan, *Matrix Computations* (Johns Hopkins University Press, Baltimore, MD, 1996).
[57] J. Grcar, "Analyses of the Lanczos Algorithm and of the Approximation Problem in Richardson's Method," Ph.D. thesis, University of Illinois, 1981.
[58] K. Wu, A. Canning, H. D. Simon, and L.-W. Wang, J. Comput. Phys. **154**, 156 (1999).
[59] K. Wu and H. D. Simon, SIAM J. Matrix Anal. Appl. **22**, 602 (2000).
[60] D. S. Sorensen, R. Lehoucq, P. Vu, and C. Yang, ARPACK, An implementation of the implicitly restarted Arnoldi iteration that computes some of the eigenvalues and eigenvectors of a large sparse matrix, 1995.
[61] J. M. Bowman, T. Carrington, Jr., and H.-D. Meyer, J. Chem. Phys. **106**, 2145 (2008).
[62] X.-G. Wang and E. L. Sibert III, J. Chem. Phys. **111**, 4510 (1999).
[63] J. L. Duncan and M. M. Law, Spectrochim. Acta, Part A **53**, 1445 (1997).
[64] L. Halonen, J. Chem. Phys. **106**, 831 (1997).
[65] E. Venuti, L. Halonen, and R. G. Della Valle, J. Chem. Phys. **110**, 7339 (1999).
[66] J. K. Xie and J. Tennyson, Mol. Phys. **100**, 1615 (2002).
[67] J. K. Xie and J. Tennyson, Mol. Phys. **100**, 1623 (2002).
[68] S. Carter, H. M. Shinder, and J. M. Bowman, J. Chem. Phys. **110**, 8417 (1999).
[69] S. Carter and J. M. Bowman, J. Phys. Chem. A **104**, 2355 (2000).
[70] T. J. Lee, J. M. L. Martin, and P. R. Taylor, J. Chem. Phys. **102**, 102 (1995).
[71] A. Chakraborty, D. G. Truhlar, J. M. Bowman, and S. Carter, J. Chem. Phys. **121**, 2071 (2004).
[72] R. Marquardt and M. Quack, J. Chem. Phys. **109**, 10628 (1998).
[73] R. Marquardt and M. Quack, J. Phys. Chem. A **108**, 3166 (2004).
[74] D. W. Schwenke and H. Partridge, Spectrochim. Acta, Part A **57**, 887 (2001).
[75] D. W. Schwenke and H. Partridge, Spectrochim. Acta, Part A **58**, 849 (2002).
[76] C. Oyanagi, K. Yagi, T. Taketsugu, and K. Hirao, J. Chem. Phys. **124**, 064311 (2006).
[77] X.-G. Wang and T. Carrington, Jr., J. Chem. Phys. **114**, 1473 (2001).
[78] J.-C. Hilico, O. Robert, M. Loete, S. Toumi, A. S. Pine, and L. R. Brown, J. Mol. Spectrosc. **208**, 1 (2001).
[79] R. Georges, M. Herman, J.-C. Hilico, and O. Robert, J. Mol. Spectrosc. **187**, 13 (1998).
[80] O. N. Ulenikov, E. S. Bekhtereva, S. V. Grebneva, H. Hollenstein, and M. Quack, Phys. Chem. Chem. Phys. **7**, 1142 (2005).